The Influence of Wet-Dry Cycling on the EIS of Q235 Carbon Steel in Seawater

Zhaohui Yang [1], Haiyang Yang [1,*], Jia Wang[2], Guoqing Ding[3], Caichang Dong[3], Qifu Zhang[4]

[1] Qingdao Research Institute for Marine Corrosion, CISRI, Qingdao 266071, China;
[2]College of Chemistry and Chemical engineering, Ocean University of China, Qingdao 266100, China;
[3] Qingdao NCS Testing and Protection Technology Co., Ltd., Qingdao 266071, China;
[4] China Iron&Steel Research Institute Group, Beijing, 100081, China
[*]E-mail: yanghaiyang2001@sina.com

In this paper, the influence of wet-dry cycling on the electrochemical impedance spectroscopy (EIS) of carbon steel is studied through indoor cyclic immersion tests and EIS. With seawater as the test medium, three different wet-dry ratios are selected. By means of the EIS results for different periods and ZView fitting, the changes in the film resistance R_f and charge transfer resistance R_{ct} are obtained. According to the results, all the impedance values of the system under wet-dry cycling conditions are less than those under seawater immersion conditions. With a decrease in the wet-dry ratio, the impedance value gradually decreases. Due to the continuous disturbance of the dynamic wet-dry process when in a corrosive environment, the diffusion layer of dissolved oxygen cannot establish a steady state, and the dissolved oxygen always maintains an unsteady high-speed mass transfer state, significantly accelerating the cathodic process.

Keywords: wet-dry cycling; carbon steel; seawater; corrosion; EIS

1. INTRODUCTION

Due to the strong corrosivity of seawater, steel used in marine engineering facilities may suffer from severe corrosion hazards [1–6]. The marine environment can be divided into different zones, including marine atmospheric zones, splash zones, tidal zones, immersion zones and sea-bottom mud zones. Regarding steel structures that reach from the sea floor and penetrate the ocean surface, such as marine oil production platforms, harbours, wharfs and sea-crossing bridges, the cyclic fluctuation of seawater in the tidal zone causes the steel surface to always be in the wet-dry state. Additionally, the sufficient supply of oxygen, temperature difference, wave impact, and constant concentration of salt remaining on the sample surface after seawater recedes makes the tidal zone a very complicated environment in terms of corrosion. Moreover, the dynamic alternating state of the tidal zone often

invalidates the protection measures of the equipment, which may greatly reduce the bearing capacities of the steel structures; thus, their normal and safe use may be affected and their service life may be shortened. Therefore, it is of great significance to study the corrosion of metal components in a dynamic alternating environment [7–12].

The corrosion extent of metal components in different locations of the tidal zone is diverse, which is caused by the variations in the corrosion environment based on the different locations in the tidal zone. One of the obvious differences is the wet-dry ratio during wet-dry cycling, that is, the ratio between the drying and immersion times is different in a wet-dry cycle. At present, there is still a lack of systematic research on the influence of the wet-dry ratio in a wet-dry environment on the corrosion behaviour of metals.

Wet-dry cycling has an important effect on the electrode process of materials, which can be studied by the electrochemical impedance spectroscopy [13–16]. Obtaining the difference between the corrosion process in the wet-dry state and the immersed state is helpful to understand the acceleration of electrochemical reactions during wet-dry cycling, thus helping to dig into the principle of the electrode reaction.

In this paper, a cyclic immersion test is used to simulate the corrosion of carbon steel in a tidal zone, and the rule governing the influence and operational mechanism of a dynamic alternating marine environment on the corrosion behaviour and corrosion resistance of carbon steel are analysed by means of the EIS of carbon steel corrosion in a wet-dry environment with different wet-dry ratios.

2. EXPERIMENTAL SECTION

The sample used in the test is Q235, and its composition is listed as follows (wt.%): C: 0.20, Si: 0.30, P: 0.040, S: 0.040, Mn: 0.30, and the rest is Fe.

The dimensions of the electrochemical sample are $\phi11.3$ mm×3 mm, with the rest of the sample sealed with epoxy resin. The sample was sequentially ground with sandpaper to 1200#, degreased with acetone, cleaned with absolute ethanol alcohol, dried with cold air, and then set aside.

In the immersion test, the sample was immersed in a beaker, and the temperature of the water bath was controlled at 25 °C. The wet-dry corrosion test was conducted in an alternating immersion test box with a controlled temperature of 25±2 °C and a relative humidity of 60%±5%. The test cycle was 60 minutes and 3 wet-dry ratios were used: W/D=1:5 (10 min/50 min), W/D=1:2 (20 min/40 min) and W/D=1:1 (30 min/30 min). Additionally, the test periods were 7 d, 14 d and 28 d, and seawater was taken from Wheat Island of Qingdao, China.

After the immersion test, the electrochemical test was performed with a three-electrode system. The auxiliary electrode was a platinum electrode, the reference electrode was a saturated calomel electrode, and the electrolyte was seawater. A Princeton PARSTAT2273 electrochemical workstation was used for EIS with the following parameters: a frequency range of 1 MHz~10 mHz and an AC excitation signal amplitude of 10 mV. The analysis software was ZView.
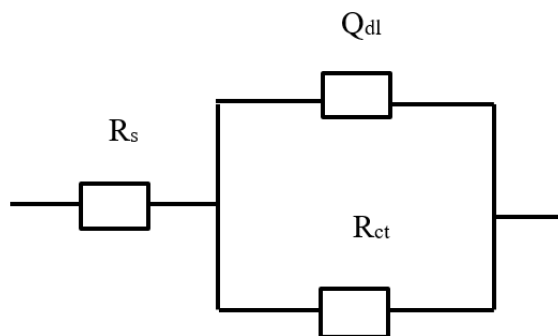
3. RESULTS AND DISCUSSION

3.1 EIS under seawater immersion conditions

The EIS results of Q235 under seawater immersion conditions are shown in Figure 1. Under seawater immersion conditions, the Nyquist diagram is a circular arc, which appears as a time constant. With increasing exposure time, the arc radius gradually increases, and no diffusion impedance appears in the low-frequency region, indicating that the electrode process is controlled by the charge transfer to the phase interface. Because the reaction is mainly the cathodic depolarization of oxygen, the process by which oxygen enters the solution and transfers mass to the electrode surface is the control step of the whole process [4, 7, 17].

According to Figure 1, the AC impedance of Q235 under seawater immersion conditions is fitted according to R_s ($Q_{dl}R_{ct}$), where R_S is the solution resistance, Q_{dl} is the constant phase angle element reflecting the electrical double-layer capacitance, and R_{ct} is the charge transfer resistance. The electrochemical parameter values obtained on the basis of the equivalent circuit are shown in Table 1.
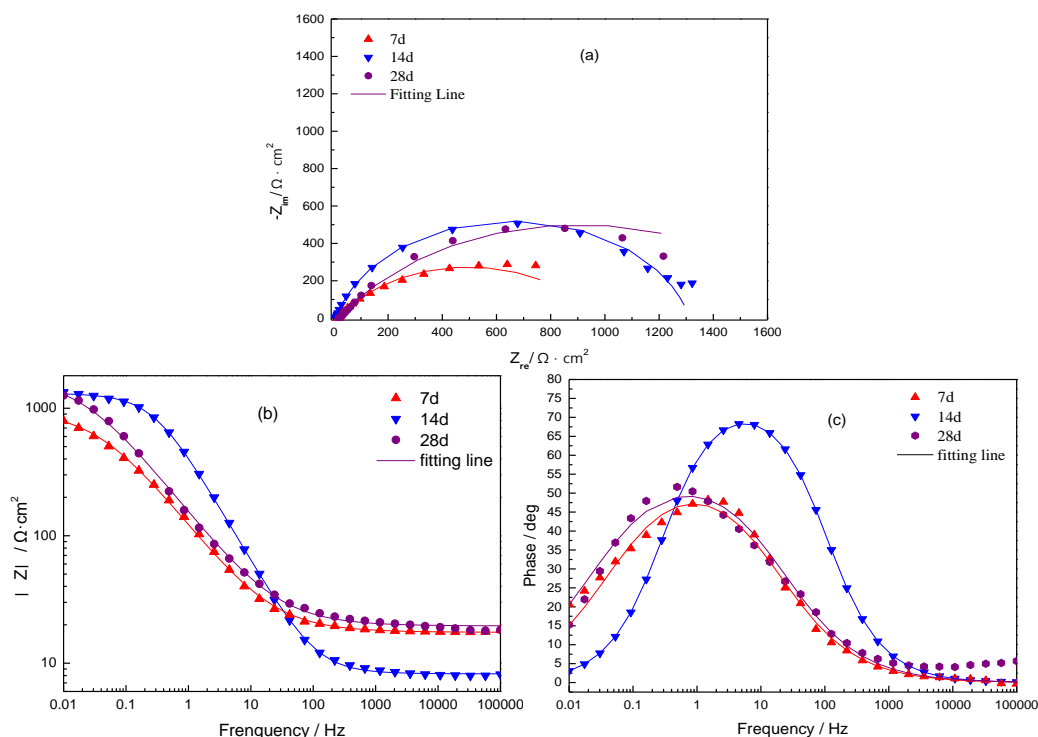
Figure 1. EIS results of Q235 under seawater immersion conditions: (a) Nyquist, (b) Bode-|Z|, and (c) Bode-Phase

Figure 2. Equivalent circuit diagram of the EIS results under seawater immersion conditions

According to the data, the resistance of the reaction when immersed mainly comes from the charge transfer resistance. With 7 d, 14 d and 28 d exposures, the values of the charge transfer resistance R_{ct} are 956 $\Omega \cdot cm2$, 1304 $\Omega \cdot cm2$ and 1769 $\Omega \cdot cm2$, respectively. Under seawater immersion conditions, the charge transfer resistance is relatively high, and during the electrode process, charge transfer through the two-phase interface between the electrode and seawater solution is relatively difficult. Within the test period, with increasing exposure time, the charge transfer resistance increases.

Table 1. Electrochemical parameters obtained from fitting under seawater immersion conditions

| Time d	R_s $\Omega \cdot cm^2$	Y_{dl} $S \cdot sec^n \cdot cm^{-2}$	n_{dl}	R_{ct} $\Omega \cdot cm^2$
7	17.48	0.002498	0.6613	956
14	8.246	0.0004596	0.8566	1304
28	19.61	0.002002	0.6547	1769

3.2 EIS under wet-dry cycling conditions

The EIS results of Q235 under the three wet-dry conditions is shown in Figures 3–5. The above electrochemical impedance results are fitted by the equivalent circuit shown in Figure 6, and the electrochemical parameters after fitting are shown in Tables 2–4.
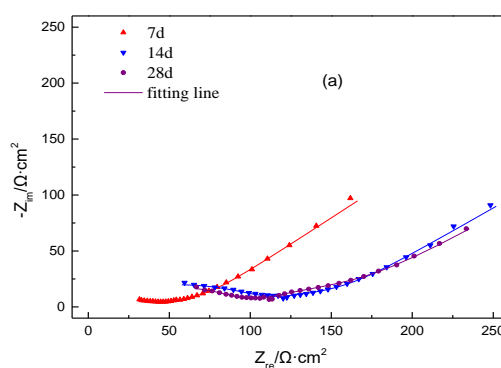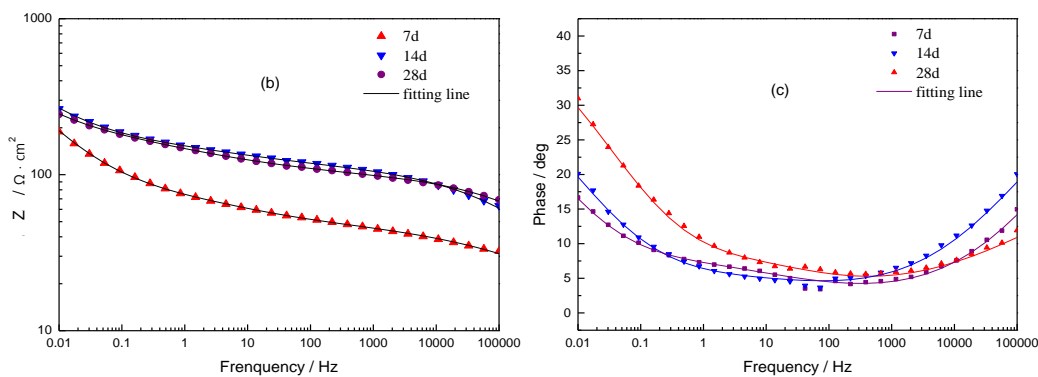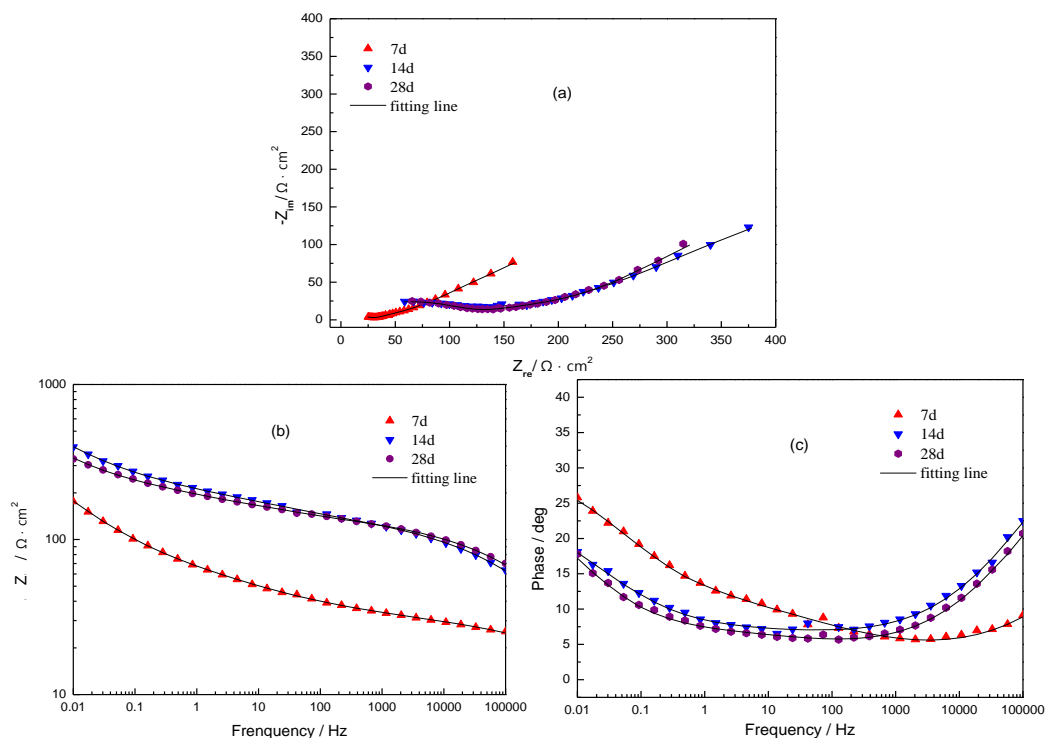
Figure 3. EIS results under the W/D= 5:1 condition: (a) Nyquist, (b) Bode-|Z|, and (c) Bode-Phase

According to Figures 3–5, the Nyquist diagrams of the samples under the three wet-dry conditions have obvious Warburg impedance diffusion tails. This result indicates that a relatively thick layer of corrosion products has formed on the carbon steel surface under these wet-dry conditions; therefore, an effect on the mass transfer diffusion process exists. Through impedance spectroscopy analysis, the film resistance and charge transfer resistance of the corrosion product layer can be obtained to study the principle of impedance under wet-dry cycling conditions.
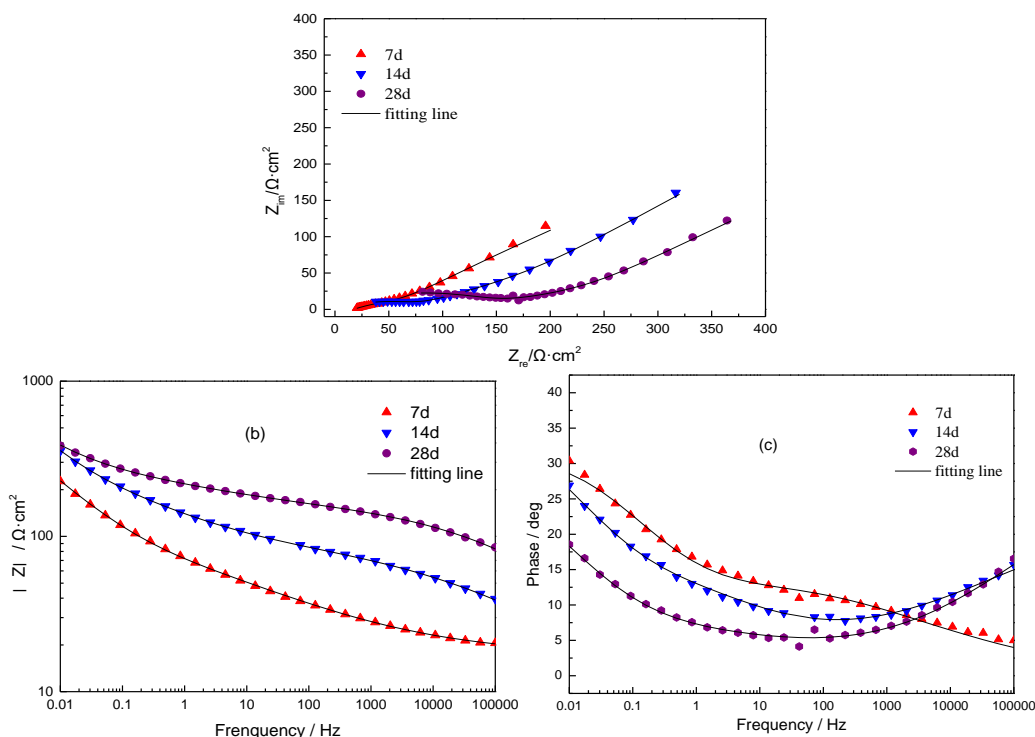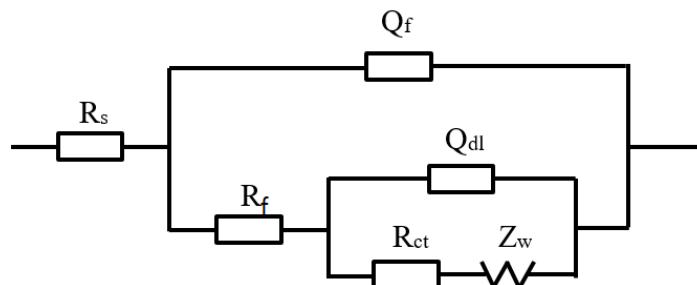

Figure 4. EIS results under the W/D=2:1 condition: (a) Nyquist, (b) Bode-|Z|, and (c) Bode-Phase

Figure 5. EIS results under the W/D=1:1 condition: (a) Nyquist, (b) Bode-|Z|, and (c) Bode-Phase

In the equivalent circuit diagram, R_S is the solution resistance, R_f is the film resistance of the corrosion product, R_{ct} is the charge transfer resistance, Z_w is the Warburg impedance of the diffusion process, Q_f is the constant phase angle element reflecting the information of the corrosion product layer, and Q_{dl} is the constant phase angle element reflecting the electrical double-layer capacitance. Q_f and Q_{dl} have two parameters: Y (capacitance admittance) and n (dimensionless index), which are marked Y_f, n_f, Y_{dl}, and n_{dl}, respectively.

Figure 6. Equivalent circuit diagram of the EIS results under the 3 wet-dry cycling conditions

Table 2. Electrochemical parameters obtained from fitting under the W/D=5:1 condition

Time d	Y_f $S \cdot sec^n \cdot cm^{-2}$	n_f	R_f $\Omega \cdot cm^2$	Y_{dl} $S \cdot sec^n \cdot cm^{-2}$	n_{dl}	R_{ct} $\Omega \cdot cm^2$	Z_W $S \cdot sec^5 \cdot cm^{-2}$
7	0.0002635	0.2943	51.17	0.007323	0.4519	35.43	0.01999
14	0.00002781	0.4281	110.80	0.006445	0.3436	81.54	0.01773
28	0.001217	0.4512	91.86	0.007316	0.2908	138.5	0.02295

Table 3. Electrochemical parameters obtained from fitting under the W/D=2:1 condition

Time d	Y_f $S \cdot sec^n \cdot cm^{-2}$	n_f	R_f $\Omega \cdot cm^2$	Y_{dl} $S \cdot sec^n \cdot cm^{-2}$	n_{dl}	R_{ct} $\Omega \cdot cm^2$	Z_W $S \cdot sec^5 \cdot cm^{-2}$
7	0.0004262	0.2644	56.52	0.007199	0.354	71.9	0.01354
14	0.0004002	0.2749	94.43	0.005625	0.4024	211.5	0.007801
28	0.00006521	0.3421	159.4	0.005894	0.3153	193.9	0.008565

Table 4. Electrochemical parameters obtained from fitting under the W/D=1:1 condition

Time d	Y_f $S \cdot sec^n \cdot cm^{-2}$	n_f	R_f $\Omega \cdot cm^2$	Y_{dl} $S \cdot sec^n \cdot cm^{-2}$	n_{dl}	R_{ct} $\Omega \cdot cm^2$	Z_W $S \cdot sec^5 \cdot cm^{-2}$
7	0.00003964	0.4073	29.59	0.01041	0.3065	109.3	0.01051
14	0.00001275	0.4854	102.80	0.003898	0.224	288.8	0.006895
28	0.00001183	0.49	80.03	0.004319	0.3055	349.9	0.01938

According to the fitting data in Tables 2–4, the rust layer does not break away from the electrode surface under the wet-dry cycling conditions, resulting in its accumulation. The corrosion product film resistance R_f exists, but all the values for the samples are small, indicating that the corrosion product film has no evident protective effect on the substrate; in fact, the corrosion product layer is less protective [17,18]. The charge transfer resistance value gradually increases with increasing wet-dry ratio, indicating that during the electrode process, the charge transfer process through the two-phase interface of the electrode and the electrolyte solution is easier under the condition of a low wet-dry ratio.

In general, the sum of the corrosion product film resistance R_f and charge transfer resistance R_{ct} is used to characterize the total resistance of the system, and the result is shown in Figure 7. When the wet-dry ratio is 5:1, the sums of these two factors for three cycles are $86.60 \Omega \cdot cm^2$, $192.34 \Omega \cdot cm^2$ and $230.36 \Omega \cdot cm^2$. When the ratio is 2:1, the sums are $128.42 \Omega \bullet cm^2$, $305.93 \Omega \bullet cm^2$ and $353.30 \Omega \bullet cm^2$. Finally, when the ratio is 1:1, the sums are $138.89 \Omega \cdot cm^2$, $391.60 \Omega \cdot cm^2$ and $429.93 \Omega \cdot cm^2$. These results show that the resistance value increases with increasing exposure time and wet-dry ratio.
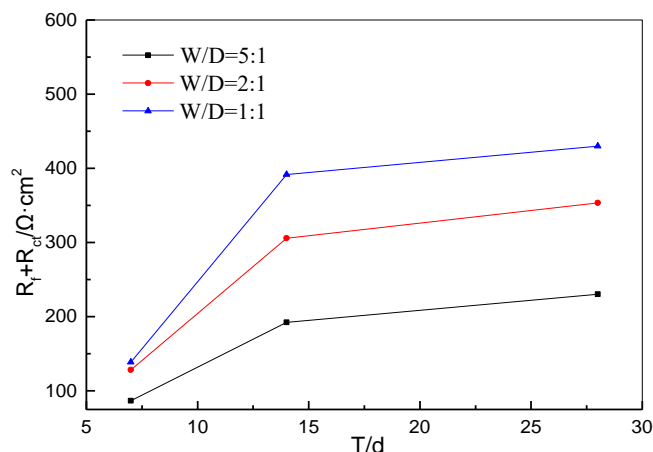
Figure 7. Diagram showing the change in the sum of the film resistance (R_f) and charge transfer resistance (R_{ct}) under the 3 wet-dry cycling conditions over time

The EIS results under seawater immersion conditions are consistent with the results of related literature [17–21]. These research results have shown that there is more γ-FeOOH and a small amount of β-FeOOH in the corrosion products under seawater immersion conditions because the potential is more conducive to the generation of γ-FeOOH. Fe_3O_4 is also generated under alternating dry and wet conditions, and β-FeOOH and Fe_3O_4 mainly exist in the inner rust layer. The higher the dry-wet ratio is, the higher the content of γ-FeOOH. Additionally, the corrosion morphology transforms from general corrosion to pitting with a decreasing wet/dry ratio.

3.3 Analysis

According to the results, there is a large difference in the corrosion behaviour during wet-dry cycling and under the immersed state, which is closely related to the influence of the liquid film on the electrode process and the active corrosion products.

Under seawater immersion conditions, the corrosion products easily break away from the corroded surface. The anodic process is the oxidation reaction of iron, while the cathodic process is the depolarization of oxygen. Oxygen diffusion is the control step of the whole reaction. According to the electrochemical results, within the three test cycles, all the charge transfer resistances are greater than 950 $\Omega \cdot cm^2$, indicating that a large resistance to the transfer of oxygen exists from the seawater solution to the electrode surface.

The drying process has a greater effect on corrosion during wet-dry cycling. Changes in the state of the liquid film occur in the drying stage, which are mainly reflected by three aspects: the change of the liquid film thickness, change of the electrolyte concentration in the liquid film and change of the liquid phase dispersion degree [22–26].

Initially during drying, the anodic and cathodic processes are simultaneously accelerated, and the cathodic reaction is primarily based on oxygen depolarization. As the liquid film thins and the electrolyte solution becomes concentrated in a wet atmosphere, oxygen is rapidly transported to the liquid film/metal interface, thereby increasing the oxygen diffusion current density and greatly increasing the

corrosion rate. Therefore, at the initial stage, the liquid film has a wide distribution area and a high degree of dispersion. Furthermore, the reactions at the three-phase interface (gas/liquid/liquid film) are active, and this process mainly accelerates the general corrosion of the material. With the formation of the rust layer, the surface corrosion products gradually accumulate. When drying, the distribution of the liquid film gradually converts to a thin liquid film. Through the cracks and pores of the corrosion products, the electrolyte solution penetrations into the interface, and oxygen passes through the thin liquid film by diffusion, thereby accelerating local corrosion of the material through depolarization.

Additionally, the corrosion mechanism transforms from oxygen depolarization to rust layer depolarization, and an oxidation-reduction reaction occurs between the rust layer and substrate, increasing the number of active sites for the cathodic reaction in the rust layer. During this process, electrochemically active γ-FeOOH and β-FeOOH participate in the cathodic depolarization reaction to form Fe_3O_4. When drying, Fe_3O_4 is oxidized to FeOOH, and Fe_3O_4 acts as a good conductor to form an electronic path, resulting in accelerated corrosion [27–35].

According to the corrosion process, under wet-dry cycling conditions, as exposure continues, the impedance value of the system increases, but due to the continuous disturbance of the dynamic wet-dry process in the corrosive environment, the diffusion layer of dissolved oxygen cannot establish a steady state, and the dissolved oxygen always maintains an unsteady high-speed mass transfer state; thus, the cathodic process is significantly enhanced. Judging from the trend of the changes in the film resistance and charge transfer resistance, the values are still small, and the impedance value of the system is significantly lower than the impedance value under seawater immersion conditions.

4. CONCLUSIONS

(1) Under three wet-dry cycling conditions, the extent of corrosion intensifies as the wet-dry ratio decreases.

(2) There is a large difference in the corrosion behaviour during wet-dry cycling and under seawater immersion conditions, which is closely related to the influence of the liquid film on the electrode process and active corrosion products.

(3) Due to the continuous disturbance of the dynamic wet-dry process in the corrosive environment, the diffusion layer of dissolved oxygen cannot establish a steady state, and the dissolved oxygen always maintains an unsteady high-speed mass transfer state, significantly accelerating the cathodic process.

References

1. X. R. Zhu, G. Q. Huang, *Corros. Sci. Protect., Tech*., 7 (1995) 246-248
2. G. Q. Huang, *Corros. Sci. Prot. Technol*., 13(2001)81-88

Int. J. Electrochem. Sci., 16 **(2021)** Article Number: 211121

10

3. S. S. Sawant, A. B. Wagh, *Corros. Prev. Contr.*, 37 (1990) 154-157
4. Y. Zou, J. Wang, Q. Bai, L. L. Zhang, X. Peng , X. F. Kong, *Corros. Sci.*, 57(2012) 202–208
5. R. Jeffrey, R. E. Melchers, *Corros. Sci.,* 51 (2009) 2291-2297
6. Z.W.Chen, W.T.Xia, C.Q.Yao, Z.F.Lin, W.Zhang, W.H.Li, *Coatings,* 10(2020)1219
7. J. G. Liu, Z. L. Li, Y. T. Li, B.R. Hou, *Int. J. Electrochem. Sci.*, 9 (2014) 8175 – 8181
8. G. A. El-Mahdy, A. Nishikata and T. Tsuru, *Corros. Sci.*, 42 (2000) 183-194
9. G. A. El-Mahdy, K.B. Kim, *Electrochim. Acta*, 49 (2004)1937-1948
10. J.H.Park, G.D.Lee, H. Ooshige, A. Nishikata, T. Tsuru, *Corros. Sci.*, 45 (2003) 1881-1894
11. B. Panda, R. Balasubramaniam, G. Dwivedi, *Corros. Sci.*, 50(2008) 1684-1692
12. M. Yamashita, H. Konishi, T. Kozakura, J. Mizuki , H. Uchida, *Corros. Sci.*, 47(2005) 2492– 2498
13. L.Bousselmi, C.Fiaud, B. Tribollets, E. Triki, *Electrochim. Acta*, 44(1999)4357-4363
14. R. E. Melchers, R. Jeffrey, *Corros. Sci.*, 45 (2003) 923-940
15. R. E. Melchers, T Wells, *Corros. Sci.*, 48 (2006) 1791-1811
16. A.Nishikata,Y.Yamashita,H.Katayama,T.Tsuru,a.Usami,K.Tanabe,H.Mabuchi, *Corros. Sci.*, 37(1995) 2059-2069
17. Q. P.Zhang, H.Y. Yang, J. Wang, Z.H. Yang, C.W. Du, *Surf. Technol.*, 49(2020)222-229
18. K. Gong, M. Wu, F. Xie, G.X. Liu, D.X. Sun, *Constr. Build. Mater.* , 260(2020)1-13
19. K.T. Kim, T. Hiroaki, H. Koushu, Y.Masato, F. Shinji, *Mater. Trans.,* 61(2020)506-514
20. J. Duboscq, R. Sabot, M. Jeannin,P. Refait. *Mater. Corros. ,* 70(2019)973-984
21. P. Refait, A.M. Grolleau, M. Jeannin, C. Rémazeilles, R. Sabot. *Corros. Mater. Degrad.,* 1(2020)198-218
22. M. Stratmann, H. Streckel, *Corros. Sci.*, 30(1990) 681-696
23. M. Stratmann, H. Streckel, *Corros. Sci.*, 30(1990) 697-714
24. M. Stratmann, *Corros. Sci.*, 27(1987) 869-872
25. N.D. Tomashov, *Corrosion*, 20 (1964) 7-14
26. A.P. Yadav, A. Nishikata, T.Tsuru, *Corros. Sci.*, 46(2004) 169-181
27. Y. H. Wang, Y. Y. Liu, W. Wang, L. Zhong, *Mater. Corros.*, 64(2013)309-313
28. Z.Y. Liu, W. K. Hao, W. Wu, H. Luo, X. G. Li, *Corros. Sci.,* 148(2019):388-396
29. U. R. Evans, C. A. J. Taylor. *Corros. Sci.,* 12 (1972) 227-246
30. S. Hoerlé, F. Mazaudier, Ph. Dillmann, G. Santarini. *Corros. Sci.*, 46(2004) 1431-1465
31. M. Stratmann, J. Miller, *Corros. Sci.*, 36(1994) 327-359
32. M. Stratmann, K. Hoffmann, *Corros. Sci.*, 29(1989) 1329-1352
33. J. Gu, Y. Xiao, N. Dai, X. Zhang, Q. Ni , J. Zhang, *Corros. Eng., Sci. Technol.*, 54(2019) 249–256
34. Y. T. Ma, Y. Li and F. H. Wang, *Mater. Chem. Phys.*, 112 (2008) 844-852
35. H.G Xiao, W.Ye, X.P.Song, Y.T.Ma, Y.Li, *Materials,* 10(2017)1262